A Physically Based Autoconversion Parameterization

HYUNHO LEE AND JONG-JIN BAIK

School of Earth and Environmental Sciences, Seoul National University, Seoul, South Korea

(Manuscript received 12 July 2016, in final form 13 February 2017)

ABSTRACT

A physically based parameterization for the autoconversion is derived by solving the stochastic collection equation (SCE) with an approximated collection kernel. The collection kernel is constructed using the terminal velocity of cloud droplets and the collision efficiency between cloud droplets that is obtained using a particle trajectory model. The new parameterization proposed in this study is validated through comparison with results obtained by a bin-based direct SCE solver and other autoconversion parameterizations using a box model. The autoconversion-related time scale and drop number concentration are employed for the validation. The results of the new parameterization are shown to most closely match those of the direct SCE solver. It is also shown that the dependency of the autoconversion rate on drop number concentration in the new parameterization is similar to that in the direct SCE solver, which is partially caused by the shape of drop size distribution. The new parameterization and other parameterizations are implemented into a cloud-resolving model, and idealized shallow warm clouds are simulated. The autoconversion parameterizations that yield the small (large) autoconversion rate tend to predict large (small) cloud optical thickness, small (large) cloud fraction, and small (large) surface precipitation amount. Cloud optical thickness and cloud fraction are changed by up to ~45% and ~20% by autoconversion parameterizations, respectively. The new parameterization tends to yield the moderate autoconversion rate among the autoconversion parameterizations. Moreover, it predicts cloud optical thickness, cloud fraction, and surface precipitation amount that are generally the closest to those of the bin microphysics scheme.

1. Introduction

Clouds provide large uncertainties in weather and climate prediction. Therefore, it is important to understand cloud processes well and reflect them accurately in numerical models. However, the size and shape of cloud particles are diverse and the microphysical processes related to cloud particles are complex, causing uncertainties and difficulties in simulating clouds and precipitation.

In warm clouds in which all cloud particles are drops, drops in clouds form from aerosol particles and grow by condensation and collision–coalescence processes. The growth of a drop by condensation tends to be slower as the drop radius is larger; it takes a few hours for a drop of radius 10 μm to grow to a drop of radius 100 μm by condensation (e.g., Pruppacher and Klett 1997). Therefore, in the growth of a droplet into a raindrop whose radius is larger than a few hundred micrometers, the collision–coalescence process plays a crucial role.

After Kessler (1969), almost all bulk cloud microphysics schemes divide drops in clouds into two categories: cloud droplets and raindrops. According to the classification, collision between drops in clouds is divided into cloud droplet–cloud droplet collision, cloud droplet–raindrop collision, and raindrop–raindrop collision. Collision between cloud droplets is again split into the self-collection and autoconversion depending on whether the formed drops are cloud droplets or raindrops, respectively. The autoconversion, which refers to collision–coalescence between cloud droplets that forms raindrops, thus plays an important role in the growth of drops in clouds. There have been many attempts to parameterize the autoconversion in bulk microphysics schemes, which are summarized in section 2.

Although the autoconversion is intrinsically the collision–coalescence between cloud droplets, most of the bulk microphysics schemes have parameterized the autoconversion based on the simple fitting to the observation data or to the results of bin microphysics schemes rather than based on the solution of the collection equation of drops. Some attempts have been made to parameterize the autoconversion based on the

Corresponding author e-mail: Jong-Jin Baik, jjbaik@snu.ac.kr

DOI: 10.1175/JAS-D-16-0207.1

analytic solution of the stochastic collection equation (e.g., Beheng and Doms 1986; Seifert and Beheng 2001).

This study parameterizes the autoconversion in terms of the collision between cloud droplets due to the difference in terminal velocities of cloud droplets, and the accurate cloud droplet collision efficiency obtained using a particle trajectory model is adopted to construct the collection kernel. A new autoconversion parameterization is derived in section 3. The experimental results from a box model and a cloud-resolving model are presented and discussed in sections 4 and 5, respectively. A summary and conclusions are given in section 6.

2. Review of previous autoconversion parameterizations

During the last several decades, many studies have been conducted to parameterize the autoconversion. Autoconversion parameterizations proposed so far can be classified into four categories: 1) parameterizations using the Heaviside function, 2) parameterizations using the time scale that is obtained by employing bin microphysics schemes, 3) parameterizations using the power-law fitting function, and 4) parameterizations obtained by solving the stochastic collection equation (SCE).

a. Parameterizations with the Heaviside function

Kessler (1969) first categorized drops in clouds into cloud droplets and raindrops in the microphysics scheme and proposed a simple parameterization of the autoconversion. The parameterization is expressed using the Heaviside function (which returns 1 if a specific quantity is larger than or equal to its threshold and 0 otherwise) for cloud water content. Hereafter, the cloud water content means the mass concentration (mass per unit volume) of cloud droplets excluding raindrops. By using the Heaviside function, the autoconversion rate is zero when the cloud water content is below the threshold value and it is linearly proportional to cloud water content when the cloud water content is larger or equal to the threshold value. The parameterization is written as

$$\left.\frac{\partial L_r}{\partial t}\right|_{\rm au} = a_{\rm Ke}(L_c - L_{c0})H(L_c - L_{c0}), \tag{1}$$

where L_r is the rainwater content (mass concentration of raindrops), $a_{\rm Ke}$ is a constant, L_c is the cloud water content, L_{c0} is the threshold value of cloud water content, and $H(x)$ represents the Heaviside function. The subscript "au" refers to the autoconversion.

Because of its simplicity, the Kessler's parameterization has been widely used in numerical models. Meanwhile, many attempts have been made to improve the Kessler's parameterization. For example, Manton and Cotton (1977) suggested $a_{\rm Ke}$ as a function of cloud droplet number concentration. Tripoli and Cotton (1980), Liou and Ou (1989), and Baker (1993) also suggested improvements upon the Kessler's parameterization. Liu and Daum (2004) provided a theoretical background for the Kessler's parameterization, showing that the Heaviside function form of the autoconversion parameterization can be derived by applying the mean value theorem to the collection equation. They suggested a generalized version of the Heaviside function form of the autoconversion parameterization by eliminating the incorrect or unnecessary assumptions; for example, the collection efficiency and the drop terminal velocity do not have to necessarily have specified forms. Also, they showed that the sixth moment of drop radius r_6 is more suitable for the threshold quantity than the cloud water content (the third moment of drop radius) if the collision kernel of Long (1974) is considered. They proposed an autoconversion parameterization (LD04) that is expressed by

$$\left.\frac{\partial L_r}{\partial t}\right|_{\rm au} = \eta_{\rm LD}\frac{L_c^3}{N_c}H(r_6 - r_{6c}) \quad \text{and} \tag{2a}$$

$$\eta_{\rm LD} = \left(\frac{3}{4\pi\rho_w}\right)^2 \kappa\beta_6^6, \tag{2b}$$

where N_c is the cloud droplet number concentration, r_{6c} is the threshold value of the sixth moment of drop radius, ρ_w is the liquid water density, κ is a constant related to the collection kernel [$1.9 \times 10^{11}\,{\rm cm^{-3}\,s^{-1}}$ in Long (1974)], and β_6 is a parameter related to the dispersion of the cloud droplet size distribution. Despite the theoretical background of LD04, however, r_{6c} still remains somewhat arbitrary. In addition, Wood and Blossey (2005) commented that LD04 contains the self-collection of cloud droplets as well as the autoconversion.

b. Parameterizations with the time scale

Berry and Reinhardt (1974) provided another parameterization of the autoconversion (BR74). In their study, a time scale of the autoconversion (i.e., the time required to satisfy the criterion for the autoconversion) is calculated as a function of mean cloud droplet radius and cloud water content using a bin microphysics scheme. By examining the produced rainwater content during the time scale, the autoconversion can be parameterized as

$$\left.\frac{\partial L_r}{\partial t}\right|_{\rm au} = \frac{L_{\rm BR}}{T_{\rm BR}}, \tag{3}$$

where $T_{\rm BR}$ is the time scale of the autoconversion and $L_{\rm BR}$ is the rainwater content at $t = T_{\rm BR}$. In BR74, $T_{\rm BR}$

and L_{BR} are represented as a function of mean cloud droplet radius and cloud water content [(16) and (18) in Berry and Reinhardt (1974)]. Because of its simple but solid parameterization obtained using a bin-based model, BR74 has been widely adopted in bulk microphysics schemes (e.g., Cohard and Pinty 2000; Milbrandt and Yau 2005; Thompson et al. 2008; Lim and Hong 2010). Note that some studies point out that BR74 contains contribution from accretion (e.g., Beheng and Doms 1986; Cohard and Pinty 2000).

c. *Parameterizations with the power-law fitting function*

Beheng (1994) first tried to derive a model-based empirical parameterization of the autoconversion as a function of cloud water content, cloud droplet number concentration, and cloud droplet size distribution parameter. Using the results of the large-eddy simulation (LES) model with a bin microphysics scheme that is designed for simulating maritime stratocumulus, Khairoutdinov and Kogan (2000) suggested an autoconversion parameterization with the power-law function (KK00). In their study, the autoconversion is parameterized in the form of

$$\left.\frac{\partial L_r}{\partial t}\right|_{au} = c_{KK}\rho_a^{1-a_{KK}} L_c^{a_{KK}} N_c^{b_{KK}}, \tag{4}$$

where ρ_a is the air density and a_{KK}, b_{KK}, and c_{KK} are constants obtained using a regression method. By applying the least squares method, the obtained values for the constants are $a_{KK} = 2.47$, $b_{KK} = -1.79$, and $c_{KK} = 1350$ when L_r, ρ_a, and L_c have units of kilograms per cubic meter and N_c has units of per cubic centimeter. This method is further used in Franklin (2008) to evaluate the effects of turbulence in the autoconversion. Note that Khairoutdinov and Kogan (2000) considered only marine stratocumulus in which the cloud water content is usually small (typically less than $1\,g\,m^{-3}$). Therefore, it is uncertain whether the parameterization can also be applied to clouds with relatively large cloud water contents. For example, Kogan (2013) showed that if the same method in Kharioudinov and Kogan (2000) is applied to the shallow cumulus, the absolute values of a_{KK} and b_{KK} become larger than those originally obtained.

d. *Parameterizations obtained by solving the stochastic collection equation*

In addition to the empirical fitting to LES model data or bin microphysics scheme results, there have been attempts to derive an analytic formula for the autoconversion from the stochastic collection of cloud droplets. Beheng (1996) proposed an approximated form of the collision efficiency given in Hall (1980) and solved SCE numerically. Using the collection kernels proposed in Long (1974) and Pinsky et al. (2001), Seifert and Beheng (2001) succeeded in deriving an analytic formula for the autoconversion, and the parameterization is further improved in Seifert and Beheng (2006). The improved parameterization (SB06) is given as

$$\left.\frac{\partial L_r}{\partial t}\right|_{au} = \frac{k_{SB}}{20m^*}\frac{(\nu+2)(\nu+4)}{(\nu+1)^2} L_c^2 \overline{m}_c^2 \left[1+\frac{\Phi(\tau)}{(1-\tau)^2}\right]\frac{\rho_{a0}}{\rho_a} \quad \text{and} \tag{5a}$$

$$\Phi(\tau) = 400\tau^{0.7}(1-\tau^{0.7})^3, \tag{5b}$$

where k_{SB} is a constant [$9.44\times10^9\,m^3\,kg^{-2}\,s^{-1}$ based on drop collision efficiencies of Pinsky et al. (2001)], m^* is the threshold mass which separates cloud droplets from raindrops (2.68×10^{-10} kg, corresponding to a drop radius of 40 μm), ν is a dispersion parameter in the cloud droplet size distribution, $\overline{m}_c$ is the mean cloud droplet mass ($=L_c/N_c$), τ is the rainwater content ratio [$=L_r/(L_c+L_r)$], and ρ_{a0} is the reference air density.

3. Derivation of a new autoconversion parameterization

In this section, a detailed description of the derivation of a new autoconversion parameterization is given. The well-known SCE that describes the change in the drop number concentration due to the collision process is given as follows:

$$\frac{\partial f(m)}{\partial t} = \int_0^{m/2} f(m')K(m', m-m')f(m-m')\,dm' - \int_0^{\infty} f(m)K(m,m')f(m')\,dm', \tag{6}$$

where $f(m)dm$ is the drop number concentration in the mass interval of [m, $m + dm$] and K is the collection kernel. The first term of the rhs of (6) represents the increase in the concentration of drops of mass m due to the collision between drops whose masses are m' and $m - m'$, while the second term represents the decrease in the concentration of drops of mass m due to the collision with other drops. The collection kernel K is expressed by the product of the swept volume of two drops per unit time and the collection efficiency as follows:

$$K(r,r') = \pi(r+r')^2|v_t(r)-v_t(r')|\eta, \tag{7}$$

where r and r' are the radii of the drops, v_t is the drop terminal velocity, and η is the collection efficiency that is the product of collision efficiency and coalescence

efficiency. In this study, the coalescence efficiency is assumed to be 1, so the collection efficiency is equal to the collision efficiency.

Because the autoconversion considers the production of raindrops via the collision between cloud droplets, the second term of the rhs of (6) is excluded to consider the autoconversion. Therefore, the autoconversion rate can be expressed using SCE as

$$\left.\frac{\partial L_r}{\partial t}\right|_{\text{au}} = \int_{m^*}^{\infty}\int_{0}^{m/2} mf(m')K(m', m-m')f(m-m')\,dm'\,dm. \tag{8}$$

The rhs of (8) can be divided into two terms as

$$\left.\frac{\partial L_r}{\partial t}\right|_{\text{au}} = \int_{0}^{\infty}\int_{0}^{m/2} mf(m')K(m', m-m')f(m-m')\,dm'\,dm - \int_{0}^{m^*}\int_{0}^{m/2} mf(m')K(m', m-m')f(m-m')\,dm'\,dm. \tag{9}$$

The second term of the rhs of (9) represents the self-collection of cloud droplets; that is, the formed drop has a mass less than m^*. By introducing the change of variables ($m' \rightarrow m$, $m - m' \rightarrow M$), (9) is given as

$$\left.\frac{\partial L_r}{\partial t}\right|_{\text{au}} = \int_{0}^{\infty}\int_{0}^{M} (M+m)f(m)K(m, M)f(M)\,dm\,dM - \int_{0}^{m^*}\int_{0}^{\hat{m}} (M+m)f(m)K(m, M)f(M)\,dm\,dM, \tag{10}$$

where $\hat{m} = \min(M, m^* - M)$. By changing the variables from mass quantities to radius quantities, (10) is rewritten as

$$\left.\frac{\partial L_r}{\partial t}\right|_{\text{au}} = \frac{4}{3}\pi\rho_w\int_{0}^{\infty}\int_{0}^{R} (R^3+r^3)f(r)K(r, R)f(R)\,dr\,dR - \frac{4}{3}\pi\rho_w\int_{0}^{r^*}\int_{0}^{\hat{r}} (R^3+r^3)f(r)K(r, R)f(R)\,dr\,dR. \tag{11}$$

Here, $\hat{r}$ is the radius of drop of mass $\hat{m}$. In this study, r^*, which is the radius that separates cloud droplets from raindrops, is set to 40 μm following BR74 and SB06.

Equation (10) is somewhat different from the expression for autoconversion proposed in Beheng and Doms (1986), in the sense that it takes account of the drops that are regarded as cloud droplets but whose masses are larger than m^* to evaluate the autoconversion. However, almost all of bulk microphysics schemes that adopt a continuous distribution defined in the radius range from zero to infinity to represent the size distribution of cloud droplet do not tend to restrict the mass of cloud droplet to m^* but tend to include all cloud droplets for calculating cloud droplet–related processes. Instead of regarding those drops as raindrops, bulk microphysics schemes have usually considered another distribution to represent raindrop size distribution. This approach is validated by showing that only a very small portion of the total cloud droplet mass is occupied by those drops (usually much smaller than 1%) and that the difference in calculated autoconversion rate is very small compared to its variance. Therefore, (10) would not be regarded as the inclusion of accretion.

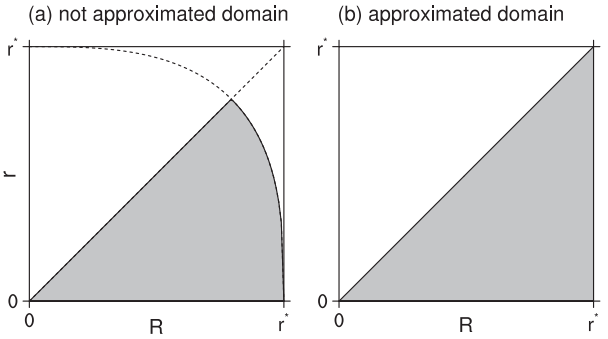

FIG. 1. (a) The integration domain of the second term on the rhs of (11) that is not approximated. (b) The integration domain of the second term on the rhs of (11) that is approximated as the second term on the rhs of (12).

It is noted that the analytical evaluation of the second term of the rhs of (11), which represents the self-collection of cloud droplets, without any approximation is too difficult because it has a complex integration domain. The integration domain is depicted in Fig. 1. By inspecting the integration domain, (11) is approximated as

$$\left.\frac{\partial L_r}{\partial t}\right|_{\text{au}} \approx \frac{4}{3}\pi\rho_w\int_{0}^{\infty}\int_{0}^{R} (R^3+r^3)f(r)K(r, R)f(R)\,dr\,dR - \alpha\frac{4}{3}\pi\rho_w\int_{0}^{r^*}\int_{0}^{R} (R^3+r^3)f(r)K(r, R)f(R)\,dr\,dR. \tag{12}$$

A constant α is introduced to avoid a slight overestimation in the approximated self-collection of cloud droplets. The constant α, which is less than but should be close to 1, is determined to be 0.88 using our bin microphysics scheme results.

Equation (12) can be evaluated if $f(r)$ and $K(r, R)$ are appropriately given. A gamma distribution is used to express $f(r)$:

$$f(r) = N_0 r^{\mu}\exp(-\lambda r), \tag{13}$$

where N_0, μ, and λ are the intercept, dispersion, and slope parameters of the gamma distribution, respectively. Many double-moment microphysics schemes

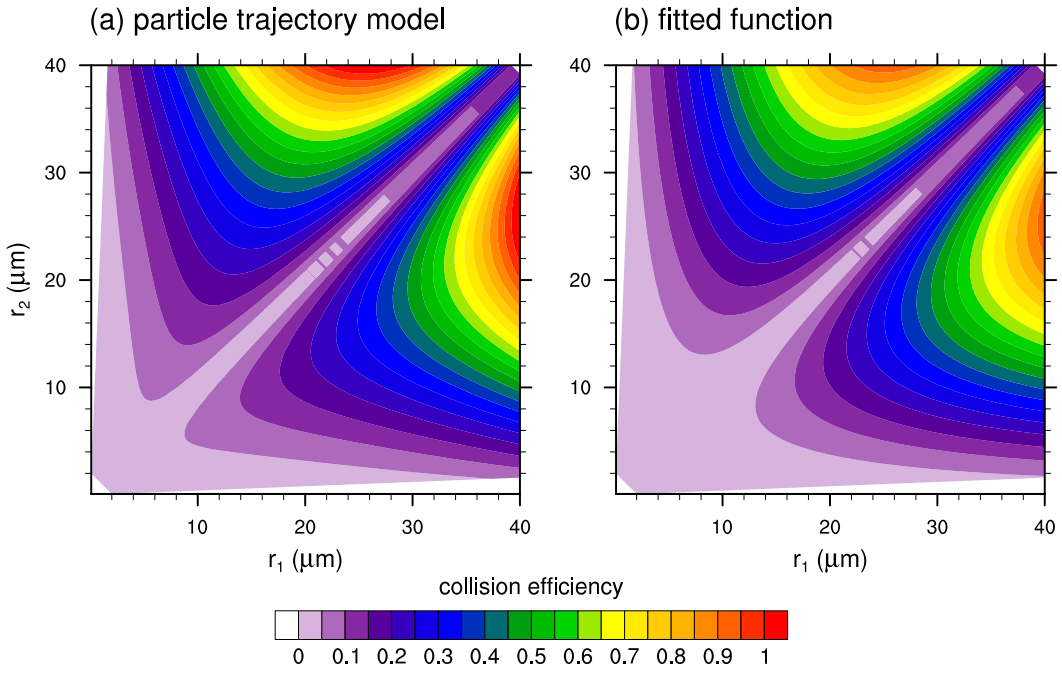

FIG. 2. Collision efficiency between cloud droplets (a) from the particle trajectory model (Pinsky et al. 2001) and (b) fitted by (14).

predict the intercept and slope parameters and set the dispersion parameter as a constant (e.g., Cohard and Pinty 2000; Seifert and Beheng 2001; Milbrandt and Yau 2005; Lim and Hong 2010). On the other hand, some double-moment microphysics schemes diagnose the dispersion parameter rather than set it as a constant (e.g., Morrison et al. 2005; Thompson et al. 2008), thereby obtaining greater reality in representing the drop size distribution. This study uses the method proposed by Thompson et al. (2008), which diagnoses the dispersion parameter $\mu = \text{nint}(10^9/N_c + 2)$, where N_c is the number concentration of cloud droplets (m^{-3}) and nint(x) returns the nearest integer of x. The maximum value of μ is limited to 15 following Thompson et al. (2008).

Therefore, if $K(r, R)$ can be expressed as a function similar to (13) or a polynomial function, (12) can be integrated analytically using the incomplete gamma function integration. In this study, a polynomial function form is adopted to represent $K(r, R)$. To represent $K(r, R)$ with a polynomial function, the collision efficiency η and the terminal velocity v_t should be fitted by polynomial functions.

To determine an expression of η, the collision efficiency obtained by adopting a particle trajectory model (Pinsky et al. 2001) is used. By observing η of Pinsky et al. (2001), a polynomial function is employed as follows:

$$\eta = k_c \frac{r}{R}\left(1 - \frac{r}{R}\right)\left(\frac{r}{R} + a\right)(R^3 + bR^4), \qquad (14)$$

where k_c, a, and b are constants to be used to fit the collision efficiency of Pinsky et al. (2001). The obtained k_c, a, and b are 1.3543×10^8, 2.1421×10^{-1}, and -1.1135×10^2 (r and R in meters), respectively. The fitted result is compared to the collision efficiency of Pinsky et al. (2001) in Fig. 2. Underestimation of the collision efficiency is seen across almost all drop sizes, particularly for very small drops. However, in general, a good agreement is shown.

The terminal velocity of drops obtained by Beard (1976) is used to determine an expression of v_t. In many previous studies, it is usual to express the terminal velocity of drops as $v_t = v_0 r^\gamma$. Figure 3 shows that for small cloud droplets whose radii are smaller than 40 μm, γ is very close to 2. The obtained v_0 for $\gamma = 2$ using the least squares method is 1.0973×10^8 when v_t and r are in meters per second and meters, respectively.

Using the expressions of η and v_t, the collection kernel [see (7)] is given as the polynomial function of r and R. Figure 4 shows the collection kernels obtained in this study, calculated directly from the collision efficiency of Pinsky et al. (2001) and the terminal velocity of Beard (1976), used in a bin microphysics scheme (Khain et al. 2011), and obtained by Long (1974). It can be easily seen that the overall distribution pattern of the collection kernel is similar to that of η. In other words, determining η in an appropriate form is important to obtain an accurate approximation of the collection kernel. The

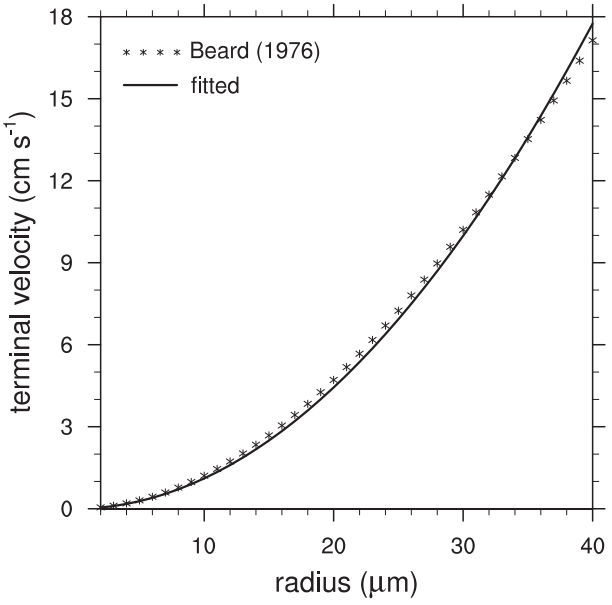

FIG. 3. Terminal velocity of cloud droplets from Beard (1976) (asterisks) and fitted to follow the Stokes's law (solid line).

collection kernel obtained in this study is much closer to the collection kernel derived from the particle trajectory model results or used in the bin microphysics scheme than the traditionally used one (Long 1974). It is noted that the collection kernels obtained in this study and used in the bin microphysics scheme are similar to each other but there are some differences between them (Figs. 4b and 4c). The values of collection kernel obtained in this study are generally smaller than those used in the bin microphysics scheme, mainly owing to the underestimation of collision efficiency. Moreover, at the diagonal, the values of collection kernel obtained in this study are zero while those used in the bin microphysics scheme are not. This is because the bin microphysics scheme uses the averaged value of collection kernel for each bin that represents a range of drop size but the values of collection kernel obtained in this study are essentially zero when the sizes of two drops are the same because their terminal velocities are the same. Despite the small differences, the collection kernels obtained in this study and used in the bin microphysics scheme are similar to each other.

The obtained collection kernel and $f(r)$ are used to evaluate the autoconversion rate [see (12)] analytically. The autoconversion rate is given as

$$\left.\frac{\partial L_r}{\partial t}\right|_{au} = \frac{4}{3}\pi^2\rho_w N_0^2 v_0 k_c (L_1 - \alpha L_2), \tag{15}$$

where

$$L_1 = \sum_{i=1}^{10} a_i \Gamma_1(\lambda, i)\left\{\Gamma_1(\lambda, 10-i) - \sum_{j=0}^{\mu+i}\frac{\lambda^j}{j!}\Gamma_1(2\lambda, 10-i+j) + b\left[\Gamma_1(\lambda, 11-i) - \sum_{j=0}^{\mu+i}\frac{\lambda^j}{j!}\Gamma_1(2\lambda, 11-i+j)\right]\right\} \quad \text{and} \tag{16a}$$

$$L_2 = \sum_{i=1}^{10} a_i \Gamma_1(\lambda, i)\left\{\Gamma_2(\lambda, 10-i) - \sum_{j=0}^{\mu+i}\frac{\lambda^j}{j!}\Gamma_2(2\lambda, 10-i+j) + b\left[\Gamma_2(\lambda, 11-i) - \sum_{j=0}^{\mu+i}\frac{\lambda^j}{j!}\Gamma_2(2\lambda, 11-i+j)\right]\right\}. \tag{16b}$$

Here, a_i $(1 \le i \le 10)$ is given as $(a, 1+a, 1-2a, -2+a, -1+2a, 2-a, -1-2a, -2+a, 1+a, 1)$, and $\Gamma_1(\lambda, n)$ and $\Gamma_2(\lambda, n)$ are defined as

$$\Gamma_1(\lambda, n) = \frac{(\mu+n)!}{\lambda^{\mu+n+1}} \quad \text{and} \tag{17a}$$

$$\Gamma_2(\lambda, n) = \Gamma_1(\lambda, n)\left[1 - e^{-\lambda r^*}\sum_{k=0}^{\mu+n}\frac{(\lambda r^*)^k}{k!}\right]; \tag{17b}$$

$(\partial L_c/\partial t)|_{au}$ is simply given as $-(\partial L_r/\partial t)|_{au}$ from the mass conservation.

The rhs of (8) with the integrand divided by m is used to evaluate the tendencies of cloud droplet number concentration and raindrop number concentration due to the autoconversion. In the autoconversion, the decrease in the number of cloud droplets is twice the number of collisions between cloud droplets, and the increase in the number of raindrops is the same as the number of collisions between cloud droplets. On the other hand, in the self-collection of cloud droplets, the decrease in the number of cloud droplets is the same as the number of collisions between cloud droplets, and there is no change in the number of raindrops. Therefore, the tendencies of cloud droplet number concentration and raindrop number concentration due to the autoconversion are expressed, respectively, as

$$\left.\frac{\partial N_c}{\partial t}\right|_{au} = -\pi N_0^2 v_0 k_c (2N_1 - \alpha N_2) \quad \text{and} \tag{18a}$$

$$\left.\frac{\partial N_r}{\partial t}\right|_{au} = \pi N_0^2 v_0 k_c (N_1 - \alpha N_2), \tag{18b}$$

where

$$N_1 = \sum_{i=1}^{7} a_i' \Gamma_1(\lambda, i)\left\{\Gamma_1(\lambda, 7-i) - \sum_{j=0}^{\mu+i}\frac{\lambda^j}{j!}\Gamma_1(2\lambda, 7-i+j) + b\left[\Gamma_1(\lambda, 8-i) - \sum_{j=0}^{\mu+i}\frac{\lambda^j}{j!}\Gamma_1(2\lambda, 8-i+j)\right]\right\} \quad \text{and} \tag{19a}$$

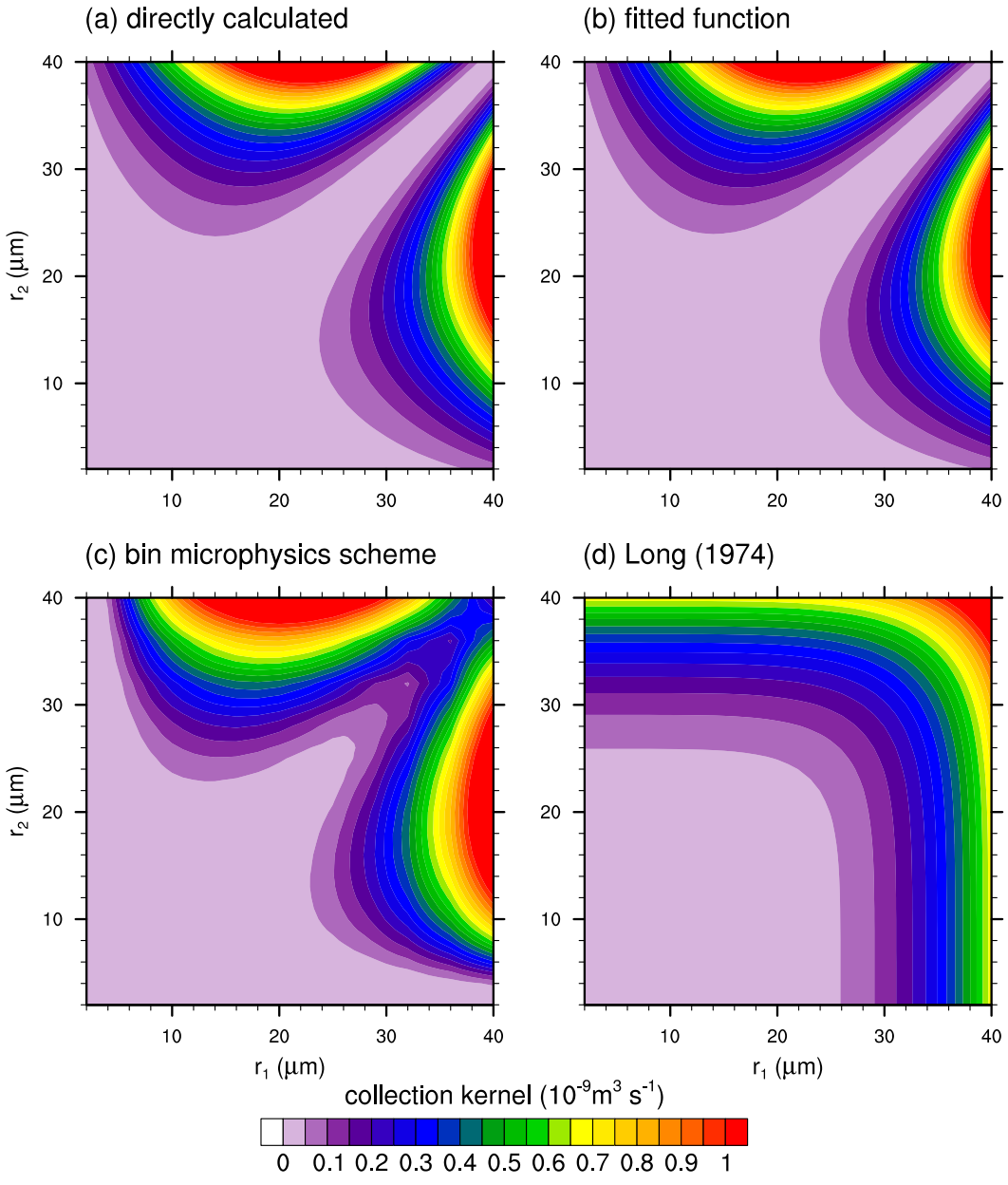

FIG. 4. Collection kernels of cloud droplets (a) directly calculated from the collision efficiency given in Pinsky et al. (2001) and the terminal velocity given in Beard (1976), (b) obtained in this study, (c) used in a bin microphysics scheme (Khain et al. 2011), and (d) proposed in an approximation form in Long (1974).

$$N_2 = \sum_{i=1}^{7} a_i' \Gamma_1(\lambda, i) \left\{ \Gamma_2(\lambda, 7-i) - \sum_{j=0}^{\mu+i} \frac{\lambda^j}{j!} \Gamma_2(2\lambda, 7-i+j) + b \left[\Gamma_2(\lambda, 8-i) - \sum_{j=0}^{\mu+i} \frac{\lambda^j}{j!} \Gamma_2(2\lambda, 8-i+j) \right] \right\}. \tag{19b}$$

Here, a_i' $(1 \le i \le 7)$ is given as $(a, 1+a, 1-2a, -2-2a, -2+a, 1+a, 1)$.

4. Box model results

The developed autoconversion parameterization is validated using a simple box model. In the box model, only the mass and number concentrations of cloud droplets are predicted, and only collision between cloud droplets is allowed. Therefore, the total liquid water mass in the box is conserved, and the mass and number concentrations of cloud droplets in the box decrease

with time by the autoconversion. For comparison, the autoconversion parameterizations BR74, KK00, LD04, and SB06 are also implemented in the box model. The original BR74 and LD04 do not provide the tendency of cloud droplet number concentration. For comparison, the decrease in cloud droplet number concentration of BR74 and LD04 due to the autoconversion is calculated using the mean cloud droplet mass (e.g., Thompson et al. 2008; Lim and Hong 2010), which is similar to that of KK00. The threshold r_{6c} used in the Heaviside function in LD04 is set to zero in this study for easier comparison. Because LD04 adopts the same gamma distribution as that in the new parameterization, the dispersion parameter μ in the distribution is diagnosed using the same method as in the new parameterization and is reflected in β_6. SB06 also utilizes the dispersion parameter [ν in (5a)], but the form of drop size distribution is slightly different from that in the new parameterization so the dispersion parameter ν is not varied and is set to zero in all simulations following Seifert and Beheng (2001).

In addition to the autoconversion parameterizations, a bin-based direct SCE solver is implemented in the box model to provide a reference. The solver uses mass-doubling bin grids in which drop masses are doubled at every three bins. There are 120 bins starting from the bin for drops whose radii are 2 μm. It is found that the bin resolution is sufficient to yield a converged solution through the comparison of the results to those obtained using 200 bins. The direct SCE solver considers drops whose radii are less than 40 μm as cloud droplets and considers only collision of cloud droplets using the exponential flux method proposed by Bott (2000). The initial drop size distribution for the solver is given as the gamma distribution [see (13)]. The model time step is set to 1 s both in the autoconversion parameterizations and in the direct SCE solver.

To evaluate the autoconversion parameterizations, the time required for 10% of the initial cloud water content to be converted into rainwater content via the autoconversion t_{10} is considered (e.g., Onishi et al. 2015). Figure 5 shows t_{10} with various initial cloud droplet number concentrations ranging from 30 to 2000 cm^{-3} and initial cloud water contents ranging from 0.25 to 2 $\mathrm{g\,m}^{-3}$. It is noted that because of the characteristics of its formula, BR74 does not yield the autoconversion rate under large cloud droplet number concentrations and small cloud water contents.

The results obtained using the new parameterization proposed in this study and LD04 are similar to the result of the direct SCE solver. BR74, KK00, and SB06 tend to diagnose generally longer t_{10} than the direct SCE solver. The new parameterization diagnoses long t_{10} compared to that of the direct SCE solver when the cloud droplet number concentration is large and the cloud water content is small. BR74 diagnoses short t_{10} under small cloud droplet number concentrations and large cloud water contents, but the increase in t_{10} with an increase in cloud droplet number concentration is very large. KK00 diagnoses substantially long t_{10} under almost all cloud droplet number concentrations and cloud water contents. It is noted that t_{10} in this study is not equal to the real time required to convert 10% of the initial cloud water content into rainwater content that might be observed in clouds, because t_{10} in this study is diagnosed by considering only autoconversion and excluding many other microphysics processes that affect the evolution of drop size distribution such as condensational growth, accretion, and sedimentation. Therefore, the box model simulation results should be carefully interpreted. A model with more microphysics parameterizations is expected to give more plausible results. It is also noted that the gamma distribution used in the new parameterization is a function of drop radius, whereas the gamma distribution used in BR74 and SB06 is a function of drop mass, which might lead to different results.

The changes in t_{10} with respect to cloud droplet number concentration in BR74, KK00, and SB06 are larger than the change in the direct SCE solver. This implies that the aerosol effects on cloud development in BR74, KK00, and SB06 might be exaggerated particularly at an early cloud developing (i.e., autoconversion dominating) stage: the decreases in autoconversion rate in BR74, KK00, and SB06 with respect to an increase in cloud droplet number concentration are generally larger than the decrease in autoconversion rate in the direct SCE solver. The changes in t_{10} with respect to cloud droplet number concentration in the new parameterization and LD04 are similar to the change in the direct SCE solver. This might be caused by using a variable dispersion parameter μ in LD04 and the new parameterization, as will be discussed.

There are some factors that can affect the results. Among them, the separation radius r^*, the constant α to control the self-collection of cloud droplets, and the dispersion parameter μ are chosen and the sensitivities of the results to those factors are examined. First, it is noted that the separation radius r^* in (11) varies depending on the autoconversion parameterization. KK00 uses r^* of 25 μm, but the other parameterizations use r^* of ~40 μm. This difference might cause an illogical comparison. However, although it is expected that the small r^* would induce a larger autoconversion rate, hence resulting in short t_{10}, Fig. 5 shows that KK00 tends to diagnose substantially long t_{10}. Therefore, it is implied that the relatively long t_{10} in KK00 is largely due to its characteristics,

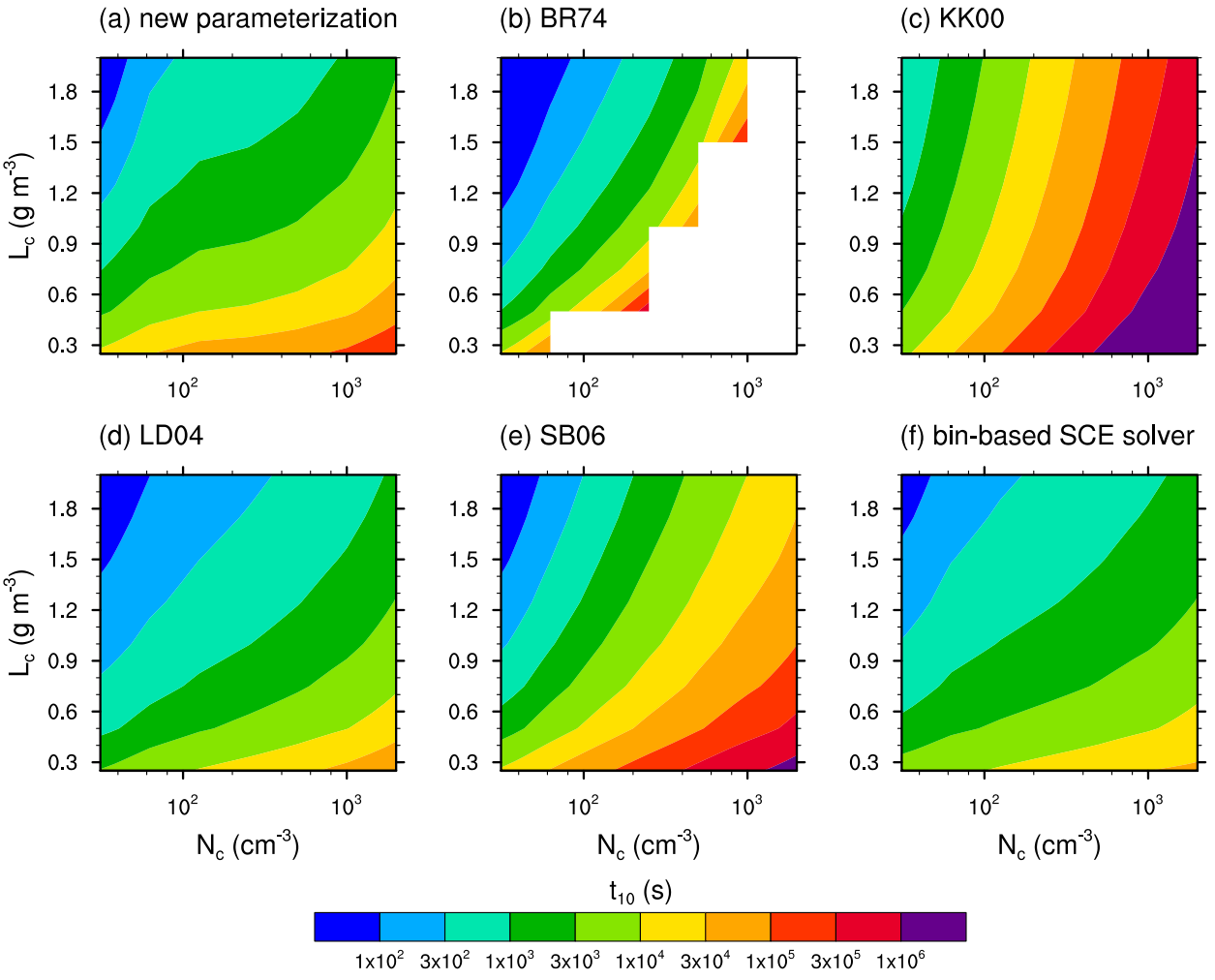

FIG. 5. Time required for 10% of the initial cloud water content to be converted into rainwater content via the autoconversion t_{10} as a function of the initial cloud droplet number concentration and cloud water content calculated using (a) the new parameterization, (b) BR74, (c) KK00, (d) LD04, (e) SB06, and (f) the bin-based SCE solver.

not due to the small r^*. In addition, sensitivity experiments to address the dependency of autoconversion on the separation radius reveal that the average change in t_{10} with r^* of 25 μm is approximately 10% in SB06, the new parameterization, and the bin-based SCE solver. The difference between the results of the two different threshold radii is generally large under small cloud droplet number concentrations and large cloud water contents, but it is very small under large cloud droplet number concentrations or small cloud water contents.

In addition, the constant α in (12) also affects the results in the new parameterization. Sensitivity experiments with different α from 0.8 to 0.99 reveal that the values of t_{10} can differ up to approximately one order. The larger α means more overestimated self-collection, hence resulting in a longer t_{10}. However, the characteristic of the changes in t_{10} with respect to cloud droplet number concentration is still shown to be similar except in the extreme case of $\alpha = 0.99$.

Sensitivity experiments with different dispersion parameter μ in (13) are also performed. In each sensitivity experiment, μ is not varied but fixed as a constant. Figure 6 shows the diagnosed t_{10} in LD04, the new parameterization, and the bin-based SCE solver with the fixed μ. In both parameterizations and the SCE solver, t_{10} increases as μ increases because a larger μ causes a narrower drop size distribution. In addition, changes in t_{10} with respect to cloud droplet number concentration in LD04, the new parameterization, and the SCE solver are different from those with varied μ and become similar to those in other parameterizations (Fig. 5). Therefore, it can be said that the characteristic of changes in t_{10} with respect to cloud droplet number concentration is somewhat affected by the dispersion parameter of the drop size distribution.

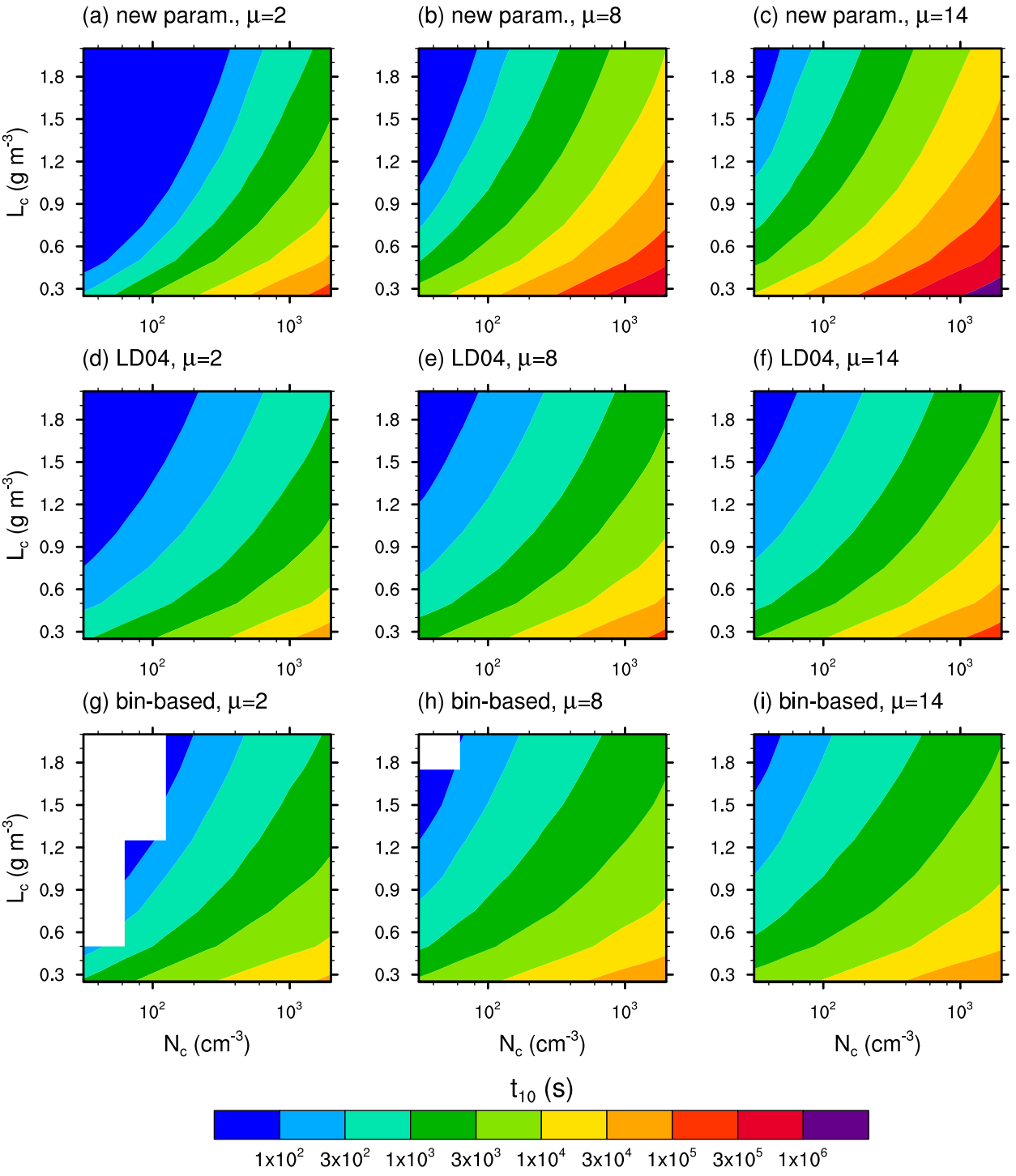

FIG. 6. (a) As in Fig. 5a, but μ is fixed to 2. (b),(c) As in (a), but μ = (b) 8 and (c) 14, respectively. (d)–(f),(g)–(i) As in (a)–(c), but for LD04 and the bin-based SCE solver, respectively.

It is noted that drops in the tail of drop size distribution can have a great influence on autoconversion. For example, in order to form a drop larger than 40 μm in radius through collision with a collected drop of 10 μm in radius, the radius of collector drop should be larger than 39.6 μm. Also, if two colliding drops have the same size, their radius should be larger than 31.8 μm to form a drop larger than 40 μm in radius. Therefore, the drops in

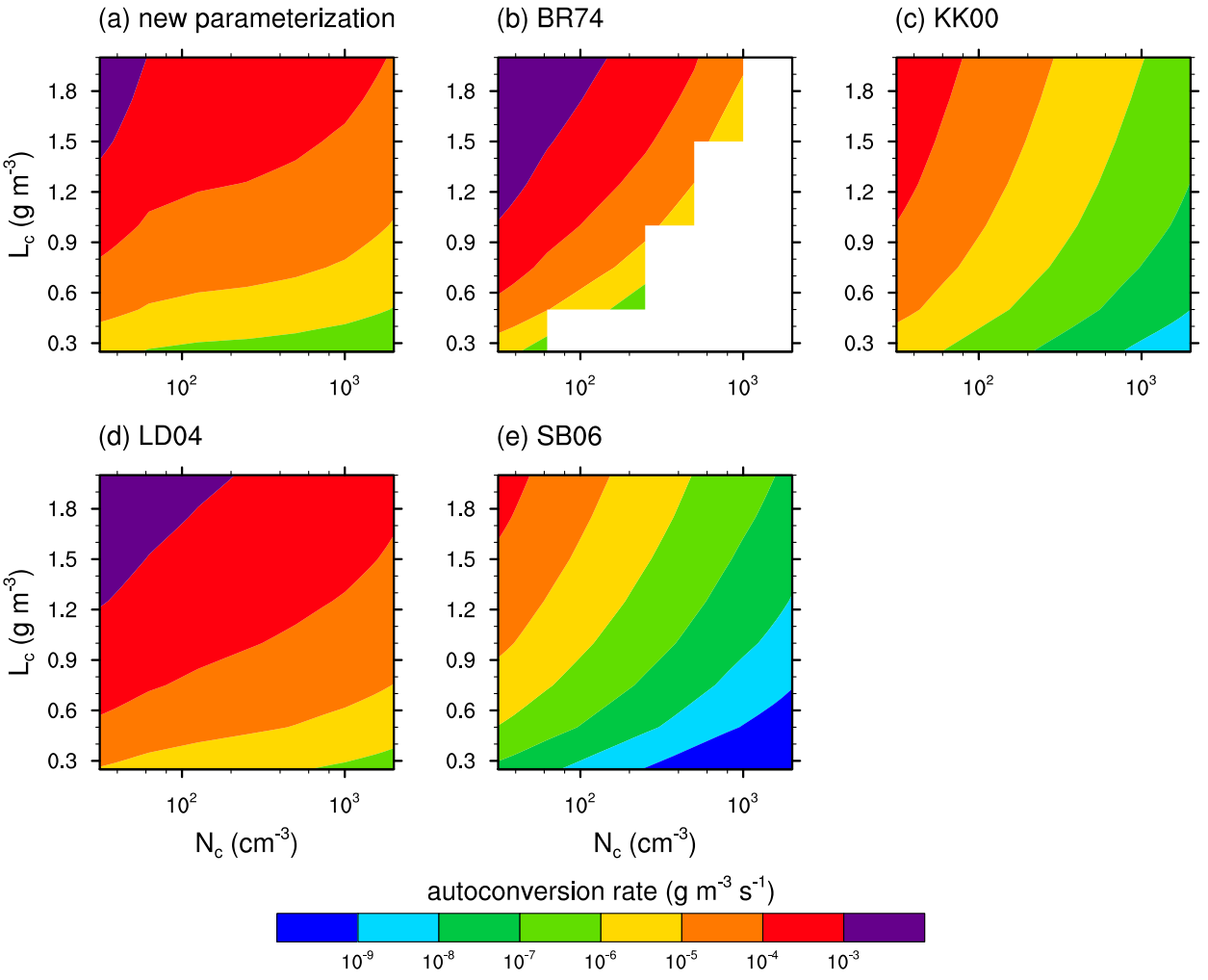

FIG. 7. As in Figs. 5a–e, but for autoconversion rate.

the tail of drop size distribution are important for autoconversion. However, there are relatively large uncertainties in representing the tail of distribution, and its representation strongly depends on the representation form of drop size distribution. In general, an autoconversion parameterization is inherently based on a specific representation form of drop size distribution and it cannot be easily altered. Further careful studies are needed to examine the effects of representation form of drop size distribution on evaluating autoconversion.

The box model used in this study considers only autoconversion to separately examine the effects of autoconversion on the evolution of drop size distribution. In reality, the collisional growth of drops occurs not only by autoconversion but also by accretion of cloud droplets by raindrops and self-collection. A series of additional box model experiments that include all the other collision processes of cloud droplets and raindrops are conducted. Analysis results show that the conversion of cloud droplets into raindrops is accelerated significantly and that the differences among the autoconversion parameterizations are reduced. Therefore, the results presented in this section should be interpreted to show only the characteristics of autoconversion depending on parameterization method, rather than to show the characteristics of whole drop growth. The effects of autoconversion parameterization with the other microphysics processes being included are examined using a cloud-resolving model in the following section.

Figure 7 shows the autoconversion rates calculated using different autoconversion parameterizations. The autoconversion rate for the bin-based solver is not given because the aspect of the time evolution of drop size distribution in bin-based solver is generally different from that in bulk autoconversion parameterizations (see Fig. 9). The general patterns of autoconversion rates are

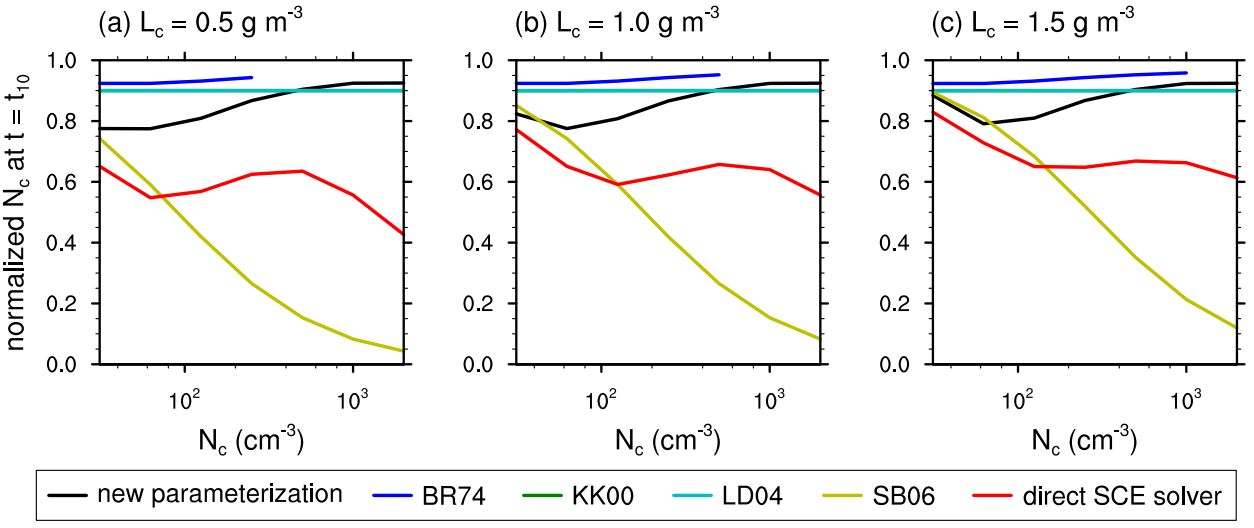

FIG. 8. Cloud drop number concentration at $t = t_{10}$ normalized by its initial value as a function of the initial cloud droplet number concentration with different autoconversion parameterizations and the bin-based direct SCE solver. The initial cloud water content is (a) 0.5, (b) 1.0, and (c) 1.5 g m^{-3}.

similar to those of t_{10}. Therefore, it can be regarded that the differences in t_{10} are mainly caused by the differences in autoconversion rates. However, there are some differences between t_{10} and autoconversion rates. For example, when the cloud droplet number concentration is large and the cloud water content is small, SB06 diagnoses t_{10} to be similar to that in the new parameterization or the direct SCE solver. However, the autoconversion rate in SB06 under these conditions is significantly smaller than that in the new parameterization.

Figure 8 shows the cloud droplet number concentration at $t = t_{10}$ normalized by its initial value under various initial cloud droplet number concentrations and initial cloud water contents calculated using different autoconversion parameterizations and the direct SCE solver. The results of KK00 and LD04 are nearly 0.9 under all initial cloud droplet number concentrations. When the initial cloud droplet number concentration is small, the deviations among the results are not so large. However, as the initial cloud droplet number concentration increases, SB06 predicts very small cloud droplet number concentration, mainly owing to the rapid self-collection of cloud droplets. This underestimation of cloud droplet number concentration in SB06 seems to compensate for the small autoconversion rates so the diagnosed t_{10} is similar to that of the direct SCE solver.

Despite overestimation, the new parameterization proposed in this study predicts the cloud droplet number concentration closest to that of the direct SCE solver among the autoconversion parameterizations. The differences between the results of the new parameterization and the direct SCE solver become smaller as the initial cloud droplet number concentration decreases and the initial cloud water content increases. The differences are large when autoconversion rates are small (i.e., large cloud droplet number concentrations and small cloud water contents). This overestimation of cloud droplet number concentration under large cloud droplet number concentrations and small cloud water contents is regarded as partially responsible for the overestimation of t_{10} (Fig. 5) by causing small autoconversion rates. In addition, the normalized cloud droplet number concentration shows a nonmonotonic behavior in the new parameterization and the SCE solver. Factors that affect the nonmonotonic behavior are not clearly grasped yet, and further studies are needed to clarify the behavior.

It is known that many autoconversion parameterizations tend to predict the time series of cloud water content different from that of bin-based SCE solver. To see this aspect, the time series of cloud water content during t_{10} is depicted in Fig. 9. Figure 9 clearly shows that all the parameterizations including the new parameterization but SB06 fail to capture the characteristic of bin-based SCE solver in which the autoconversion is accelerated. It might be postulated that the consideration of rainwater content is crucial for capturing the characteristic, so further development is vital.

5. Cloud-resolving model results

To examine improvements in numerical cloud simulation, the autoconversion parameterization developed in this study is implemented in a cloud-resolving model.

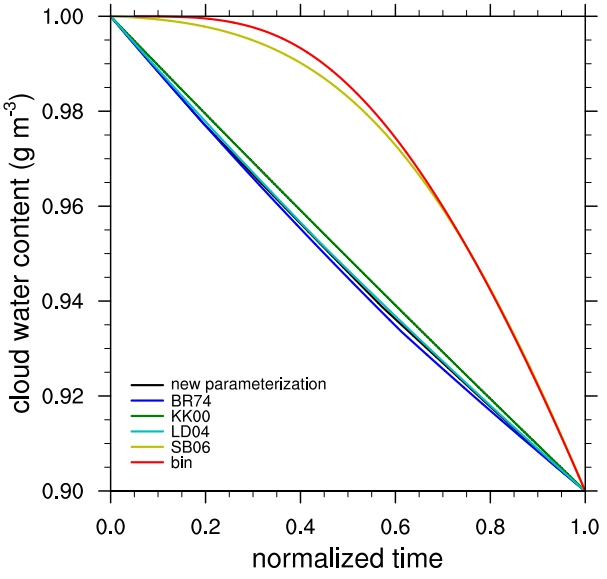

FIG. 9. Cloud water content as a function of time normalized by t_{10}. The initial cloud droplet number concentration is 100 cm^{-3} and the cloud water content is 1 g m^{-3}.

The Weather Research and Forecasting (WRF) Model, version 3.7.1 (Skamarock et al. 2008), and the Thompson microphysics scheme (Thompson and Eidhammer 2014) in the WRF Model are chosen, and the developed autoconversion parameterization is implemented in the model. In addition, the autoconversion parameterizations KK00, LD04, and SB06 are also incorporated into the model for comparison. It is noted that the Thompson microphysics scheme originally adopts the autoconversion parameterization BR74. Except for the autoconversion, all the other microphysical processes are identical to those in the Thompson microphysics scheme. Moreover, to provide a reference, the warm version of a bin microphysics scheme (Hebrew University Cloud Model; Khain et al. 2011) is coupled with the WRF Model.

A series of idealized cloud simulations that simulate shallow warm clouds are performed. The domain size is 18 km × 18 km × 4.2 km, and the grid size is 100 m in the horizontal and 30 m in the vertical. Periodic boundary conditions are applied in both the x and y directions. The sponge layer is located from $z = 3.4$ km to the domain top. A constant surface heat flux of 1.2×10^{-2} K m s^{-1} and a constant surface water vapor flux of 3.4×10^{-5} m s^{-1} (approximately 15 and 100 W m^{-2}, respectively) are applied for bottom boundary conditions. Random perturbations of [−0.3 K, 0.3 K] are added to the initial potential temperature field at the lowest four levels of the model domain. The model is integrated for 6 h with a time step of 1 s, and the results in the last 3 h are analyzed. The thermodynamic sounding is based on Ogura and Takahashi (1973), which is expressed as

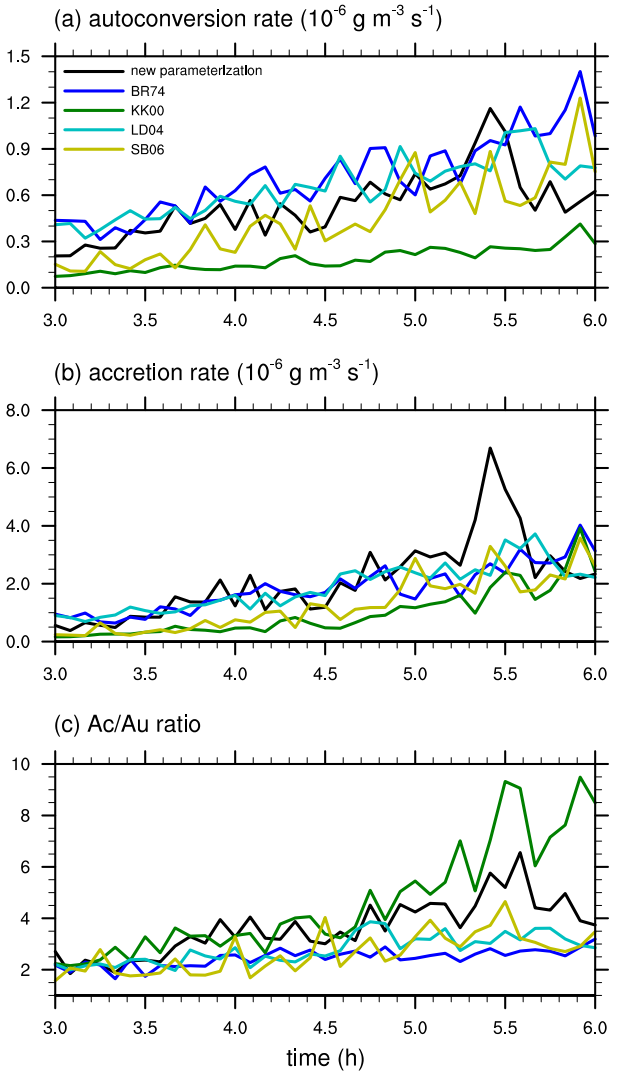

FIG. 10. Time series of (a) autoconversion rate, (b) accretion rate, and (c) the ratio of accretion rate to autoconversion rate averaged over the domain with different autoconversion parameterizations.

$$\frac{\partial T}{\partial z} = \begin{cases} -9.7\ \mathrm{K\,km^{-1}} & \text{for} \quad 0 < z < 600\ \mathrm{m} \\ -5.8\ \mathrm{K\,km^{-1}} & \text{for} \quad 600\ \mathrm{m} < z < 3\ \mathrm{km} \\ 10\ \mathrm{K\,km^{-1}} & \text{for} \quad 3 < z < 3.4\ \mathrm{km} \\ -5\ \mathrm{K\,km^{-1}} & \text{for} \quad z > 3.4\ \mathrm{km} \end{cases} \quad \text{and} \tag{20a}$$

$$\frac{\partial \mathrm{RH}}{\partial z} = \begin{cases} 10\%\ \mathrm{km^{-1}} & \text{for} \quad 0 < z < 600\ \mathrm{m} \\ -14.6\%\ \mathrm{km^{-1}} & \text{for} \quad 600\ \mathrm{m} < z < 3\ \mathrm{km} \\ -200\%\ \mathrm{km^{-1}} & \text{for} \quad 3 < z < 3.4\ \mathrm{km} \\ -15\%\ \mathrm{km^{-1}} & \text{for} \quad z > 3.4\ \mathrm{km} \end{cases}, \tag{20b}$$

where T is the air temperature (K) and RH is the relative humidity (%). The air temperature and surface

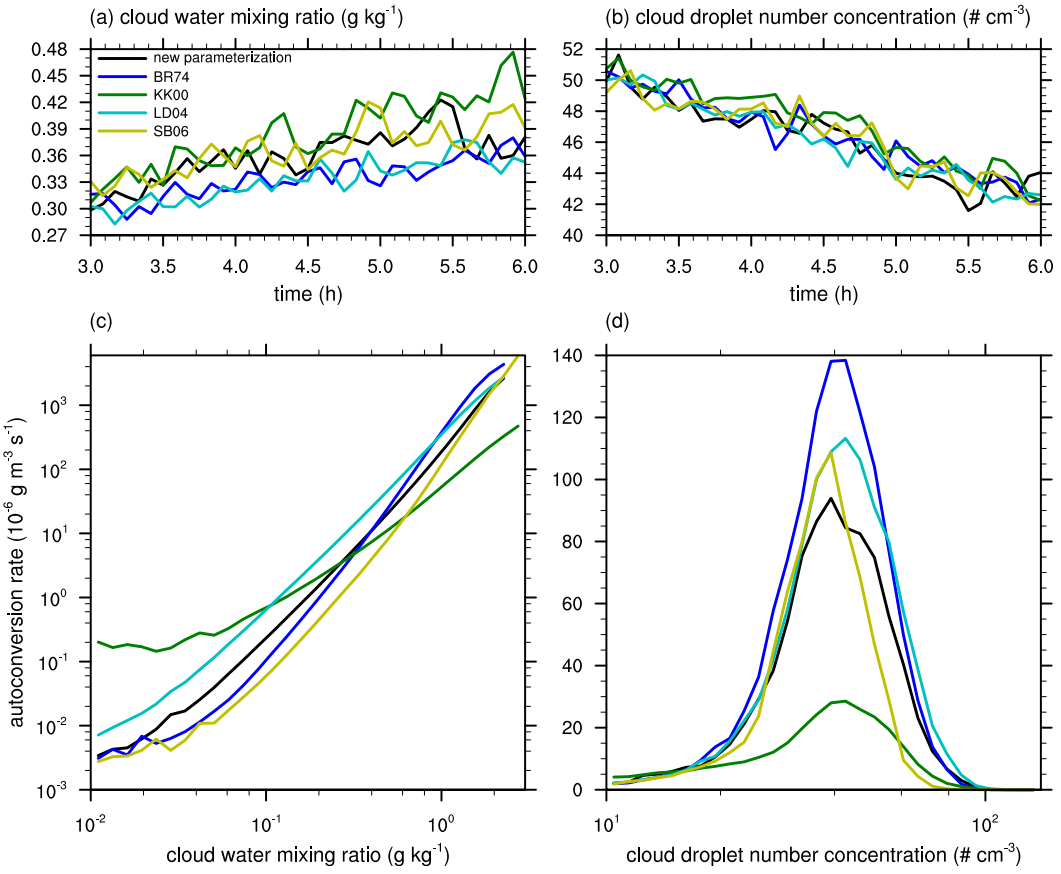

FIG. 11. Time series of (a) cloud water mixing ratio and (b) cloud droplet number concentration averaged over the cloudy grid points, and the averaged autoconversion rate expressed as a function of (c) cloud water mixing ratio and (d) cloud droplet number concentration.

relative humidity at the surface is 298.15 K and 85%, respectively. The minimum relative humidity in the upper layer is set to 10%. Note that an inversion layer exists between $z = 3$ and 3.4 km. The aerosol concentration near the surface is set to 300 cm^{-3}.

Figure 10 shows the time series of autoconversion rate, accretion rate, and ratio of accretion rate to autoconversion rate (Ac/Au ratio) averaged over the domain with the different autoconversion parameterizations. The accretion is dominant over the autoconversion in all cases: the Ac/Au ratio is in the range from 1 to 10 in all parameterizations. According to Michibata and Takemura (2015), the Ac/Au ratio is as small as 0.1 in the Heaviside function–type parameterizations. They noted that ignoring low autoconversion rate due to the threshold in the Heaviside function–type parameterizations causes overestimated autoconversion rate and underestimated Ac/Au ratio. In this study, the threshold in LD04 is set to zero, so the Ac/Au ratio of LD04 in this study is larger than that in Michibata and Takemura (2015) owing to the inclusion of low autoconversion rate.

The averaged autoconversion rate obtained using the new parameterization is generally smaller than the averaged autoconversion rates in BR74 and LD04 and generally larger than those in KK00 and SB06. The accretion rate tends to be larger for the larger autoconversion rate. This implies that while the large autoconversion rate can cause both enhanced accretion due to the increase in rainwater content and suppressed accretion due to the decrease in cloud water content, the effect of the increase in rainwater content is larger than the effect of the decrease in cloud water content. The Ac/Au ratio tends to be larger for the smaller autoconversion rate. BR74 generally shows the smallest Ac/Au ratio. KK00 generally shows the smallest autoconversion rate that results in the largest Ac/Au ratio (up to ~10), which is similar to the result of Michibata and Takemura (2015). The new parameterization shows moderate autoconversion rate, somewhat large accretion rate, and somewhat large Ac/Au ratio (between ~2 and 7).

Figure 11 shows the time series of cloud water mixing ratio and cloud droplet number concentration averaged

over the cloudy grid points at which the cloud water mixing ratio is larger than 0.01 g kg^{-1} and the averaged autoconversion rate as a function of cloud water mixing ratio and cloud droplet number concentration. The cloud water mixing ratio is relatively large in KK00 and SB06, and relatively small in BR74 and LD04, mainly because KK00 and SB06 tend to yield smaller autoconversion rate so the growth of cloud droplet to raindrop is less active, whereas BR74 and LD04 tend to yield larger autoconversion rate so the growth of cloud droplet to raindrop is more active. The cloud water mixing ratio in the new parameterization is moderate. Differences in cloud droplet number concentrations among the autoconversion parameterizations are very small.

The autoconversion rate as a function of cloud water mixing ratio shows that all the autoconversion parameterizations except KK00 are in a similar trend. LD04 shows the largest autoconversion rate among the parameterizations, and BR74 shows the largest sensitivity of the autoconversion rate to cloud water mixing ratio which is expressed by the largest slope. KK00 shows a substantially small sensitivity of the autoconversion rate to cloud water mixing ratio compared to the other parameterizations. This is mainly because KK00 is designed for marine stratocumulus, as discussed in Kogan (2013). The sensitivity of cloud droplet number concentration to the autoconversion rate is also the smallest in KK00 and the largest in BR74.

For the comparison of cloud properties, cloud optical thickness, cloud fraction, and accumulated surface precipitation amount are chosen, and their time series are plotted in Fig. 12. For comparison, the results obtained using the bin microphysics scheme are also included in Fig. 12. Cloud optical thickness is parameterized using cloud droplet number concentration and liquid water path as in Zhang et al. (2005) in the cases with the bulk microphysics schemes, but it is directly calculated in the case with the bin microphysics scheme. Cloudy column, which is used to calculate the averaged cloud optical thickness and cloud fraction, is defined as the column with a liquid water path larger than 10 g m^{-2}.

For cloud optical thickness, the new parameterization yields the cloud optical thickness closest to that in the bin microphysics scheme. BR74 and LD04, in which the autoconversion rate is large and the Ac/Au ratio is small, underestimate cloud optical thickness. On the other hand, KK00, in which the autoconversion rate is small and the Ac/Au ratio is large, overestimates cloud optical thickness. In the cases in which the autoconversion rate is large, the accretion rate also tends to be large (Fig. 10). Thus, the conversion of cloud droplets into raindrops becomes active. Therefore, the liquid water path is reduced owing to the sedimentation of raindrops, hence yielding small liquid water path and small cloud optical thickness.

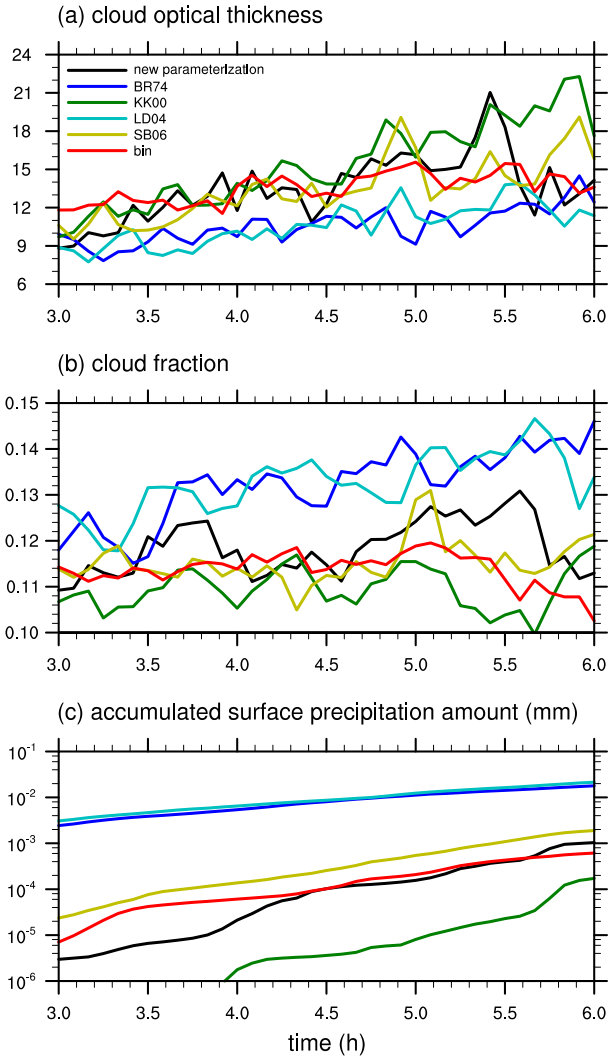

FIG. 12. Time series of (a) cloud optical thickness, (b) cloud fraction, and (c) accumulated surface precipitation amount with different autoconversion parameterizations and the bin microphysics scheme. Cloud optical thickness is averaged over the cloudy column, where liquid water path is larger than 10 g m^{-2}, and surface precipitation amount is averaged over the domain.

The parameterization proposed in this study, together with SB06, also yields the cloud fraction that is close to that in the bin microphysics scheme. KK00 underestimates cloud fraction, mainly because of facilitated evaporation due to large cloud water content and small rainwater and less dynamic enhancement due to reduced surface precipitation and resultant reduced cold pools. BR74 and LD04 show overestimated cloud fraction mainly due to the small cloud water content and large rainwater content that suppress evaporation. The accumulated surface precipitation amount is small for

TABLE 1. Cloud optical thickness (COT) and cloud fraction (CF) averaged for the last 3 h of the simulation and accumulated surface precipitation amount (PREC; 10^{-3} mm) for the last 3 h of the simulation with different autoconversion parameterizations and the bin microphysics scheme. Cloud optical thickness is averaged over the cloudy column where liquid water path is larger than 10 g m^{-2}, and 3-h accumulated surface precipitation is averaged over the domain. The relative deviation from the bin microphysics scheme result ($f/f_{\text{bin}} - 1$) is given in parentheses.

	New parameterization	BR74	KK00	LD04	SB06	Bin
COT	13.5 (−0.3%)	10.6 (−21.8%)	15.4 (13.8%)	10.6 (−21.7%)	13.4 (−0.7%)	13.5
CF	0.119 (4.2%)	0.132 (16.3%)	0.110 (−3.7%)	0.133 (16.5%)	0.115 (1.4%)	0.114
PREC	1.03 (70.4%)	15.5 (2453.0%)	0.172 (−71.6%)	18.3 (2925.3%)	1.88 (209.3%)	0.606

all cases, but it is sensitive to the autoconversion parameterization (Fig. 12c). The difference in accumulated surface precipitation amount between LD04 (the largest) and KK00 (the smallest) is more than an order of 2. Because KK00 yields the smallest autoconversion rate and the smallest total conversion of cloud droplets into raindrops, surface precipitation is suppressed by the decreased rainwater content. The reverse is the cases of BR74 and LD04. As in the cloud optical thickness and cloud fraction, the new parameterization and SB06 yield the accumulated surface precipitation amount closest to that in the bin microphysics scheme. While SB06 steadily overestimates the accumulated surface precipitation amount by approximately twice that in the bin microphysics scheme, the accumulated surface precipitation amount obtained using the new parameterization becomes similar to that in the bin microphysics scheme as the model integration progresses.

Table 1 lists the cloud optical thickness and cloud fraction averaged for the last 3 h of the simulation and the accumulated surface precipitation amount for the same period with different autoconversion parameterizations and the bin microphysics scheme. The conclusions given above are thus shown in a simpler way: the results obtained using the autoconversion parameterization proposed in this study are the closest to those obtained using the bin microphysics scheme, followed by those obtained using SB06. KK00 with the smallest autoconversion rate overestimates the cloud optical thickness and underestimates the cloud fraction and surface precipitation amount, which is largely due to the underestimated rainwater content. In contrast to KK00, BR74 and LD04 underestimate the cloud optical thickness and overestimate the cloud fraction and surface precipitation amount due to the large autoconversion rate.

It should be emphasized that different autoconversion parameterizations can induce large changes in cloud properties: up to ~45% change in cloud optical thickness and ~20% change in cloud fraction for the conditions considered in this study. Moreover, the sensitivity of surface precipitation amount to autoconversion parameterization is considerably large, although surface precipitation amount is small. In this regard, Hill et al. (2015) also showed that the precipitation susceptibility is sensitive to the autoconversion parameterization, particularly when the employed microphysics scheme is single moment.

It is noted that although the new autoconversion parameterization proposed in this study is more complex than other traditional autoconversion parameterizations, the total increase in model calculation time by replacing the traditional ones with the new one is not large. For the warm cloud simulations described above, the increase in model calculation time does not exceed 3%−4%.

6. Summary and conclusions

This study derives a new physically based autoconversion parameterization by solving SCE based on the difference in terminal velocities of cloud droplets and the collision efficiency between cloud droplets obtained using a particle trajectory model. The new parameterization proposed in this study is more complex but more physically based than traditional autoconversion parameterizations. Some studies have discussed the applicability of microphysics parameterizations to various environmental conditions (e.g., Shipway and Hill 2012; Hill et al. 2015). The new parameterization is expected to be applied to various environmental conditions. An increase in total calculation time by replacing the traditional autoconversion parameterizations with the new parameterization is not large, so the efficiency of the bulk microphysics scheme is not vitiated.

Using a box model, the new parameterization was validated through comparison with the results obtained by a bin-based direct SCE solver and many traditional autoconversion parameterizations. When t_{10}, which is the time required for 10% of the initial cloud water mass to be converted into rainwater mass via the autoconversion, is employed for comparison, the new parameterization result shows one of the best agreements with that obtained using the bin-based direct SCE solver. In addition to the time scale, the new

parameterization also predicts the cloud droplet number concentration closest to that obtained using the direct SCE solver. While some autoconversion parameterizations tend to overestimate the changes in autoconversion rate due to the changes in cloud droplet number concentration, the new parameterization does not show such overestimated dependency on cloud droplet number concentration, which might be important in aerosol–cloud interaction research.

The new parameterization proposed in this study was implemented in a bulk microphysics scheme in a cloud-resolving model and was used to simulate shallow warm clouds. To provide a reference, the warm version of a bin microphysics scheme was also implemented in the same model. The new parameterization tends to yield moderate autoconversion rate and the cloud properties closest to those obtained using the bin microphysics scheme among the tested autoconversion parameterizations. This should be carefully interpreted because the environmental condition considered in this study is suitable only for shallow warm clouds under only one aerosol number concentration setting, although the box model results imply that the new parameterization might yield results closest to those obtained using the bin microphysics scheme across a wide range of aerosol number concentrations. In the autoconversion parameterization with large autoconversion rate, the accretion rate is also generally large, so is the total conversion of cloud droplets into raindrops. For cloud optical thickness, cloud fraction, and surface precipitation amount, the results of the new parameterization are generally the closest to those of the bin microphysics scheme. The autoconversion parameterizations that yield small autoconversion rates predict large cloud optical thickness, small cloud fraction, and small surface precipitation amount mainly because of the underestimated rainwater content. On the contrary, the autoconversion parameterizations that yield large autoconversion rates predict small cloud optical thickness, large cloud fraction, and large surface precipitation amount mainly as a result of the overestimated rainwater content.

This study shows that different autoconversion parameterizations can induce large changes in cloud properties. Changes in cloud optical thickness and cloud fraction due to change in autoconversion parameterization are up to ~45% and ~20%, respectively. Surface precipitation amount is also sensitive to autoconversion parameterization. Thus, an accurate parameterization of the autoconversion is important.

It is expected that the new autoconversion parameterization proposed in this study can be utilized in weather and climate models. Moreover, the strategy used in this study to parameterize the autoconversion is expected to be utilized to parameterize other collision processes (e.g., drop–graupel collision) to improve bulk microphysics schemes.

Acknowledgments. The authors are grateful to three anonymous reviewers for providing valuable comments on this study. The authors were supported by the Korea Meteorological Administration Research and Development Program under Grant KMIPA 2015-5190.

REFERENCES

Baker, M. B., 1993: Variability in concentrations of CCN in the marine cloud-top boundary layer. *Tellus*, **45B**, 458–472, doi:10.3402/tellusb.v45i5.15742.

Beard, K. V., 1976: Terminal velocity and shape of cloud and precipitation drops aloft. *J. Atmos. Sci.*, **33**, 851–883, doi:10.1175/1520-0469(1976)033<0851:TVASOC>2.0.CO;2.

Beheng, K. D., 1994: A parameterization of warm cloud microphysical conversion processes. *Atmos. Res.*, **33**, 193–206, doi:10.1016/0169-8095(94)90020-5.

——, 1996: An approximation formula for drop/drop-collision efficiencies. *Proc. 12th Int. Conf. on Clouds and Precipitation*, Zurich, Switzerland, International Commission on Clouds and Precipitation, 917–920.

——, and G. Doms, 1986: A general formulation of collection rates of clouds and raindrops using the kinetic equation and comparison with parameterizations. *Contrib. Atmos. Phys.*, **59**, 66–84.

Berry, E. X., and R. L. Reinhardt, 1974: An analysis of cloud drop growth by collection: Part II. Single initial distributions. *J. Atmos. Sci.*, **31**, 1825–1831, doi:10.1175/1520-0469(1974)031<1825:AAOCDG>2.0.CO;2.

Bott, A., 2000: A flux method for the numerical solution of the stochastic collection equation: Extension to two-dimensional particle distributions. *J. Atmos. Sci.*, **57**, 284–294, doi:10.1175/1520-0469(2000)057<0284:AFMFTN>2.0.CO;2.

Cohard, J.-M., and J.-P. Pinty, 2000: A comprehensive two-moment warm microphysical bulk scheme. I: Description and tests. *Quart. J. Roy. Meteor. Soc.*, **126**, 1815–1842, doi:10.1256/smsqj.56613.

Franklin, C. N., 2008: A warm rain microphysics parameterization that includes the effect of turbulence. *J. Atmos. Sci.*, **65**, 1795–1816, doi:10.1175/2007JAS2556.1.

Hall, W. D., 1980: A detailed microphysical model within a two-dimensional dynamic framework: Model description and preliminary results. *J. Atmos. Sci.*, **37**, 2486–2507, doi:10.1175/1520-0469(1980)037<2486:ADMMWA>2.0.CO;2.

Hill, A. A., B. J. Shipway, and I. A. Boutle, 2015: How sensitive are aerosol-precipitation interactions to the warm rain representation? *J. Adv. Model. Earth Syst.*, **7**, 987–1004, doi:10.1002/2014MS000422.

Kessler, E., 1969: *On the Distribution and Continuity of Water Substance in Atmospheric Circulations. Meteor. Monogr.*, No. 32, Amer. Meteor. Soc., 88 pp.

Khain, A., D. Rosenfeld, A. Pokrovsky, U. Blahak, and A. Ryzhkov, 2011: The role of CCN in precipitation and hail in a mid-latitude storm as seen in simulations using a spectral (bin) microphysics model in a 2D dynamic frame. *Atmos. Res.*, **99**, 129–146, doi:10.1016/j.atmosres.2010.09.015.

Khairoutdinov, M., and Y. Kogan, 2000: A new cloud physics parameterization in a large-eddy simulation model of marine stratocumulus. *Mon. Wea. Rev.*, **128**, 229–243, doi:10.1175/1520-0493(2000)128<0229:ANCPPI>2.0.CO;2.

Kogan, Y., 2013: A cumulus cloud microphysics parameterization for cloud-resolving models. *J. Atmos. Sci.*, **70**, 1423–1436, doi:10.1175/JAS-D-12-0183.1.

Lim, K.-S. S., and S.-Y. Hong, 2010: Development of an effective double-moment cloud microphysics scheme with prognostic cloud condensation nuclei (CCN) for weather and climate models. *Mon. Wea. Rev.*, **138**, 1587–1612, doi:10.1175/2009MWR2968.1.

Liou, K.-N., and S.-C. Ou, 1989: The role of cloud microphysical processes in climate: An assessment from a one-dimensional perspective. *J. Geophys. Res.*, **94D**, 8599–8607, doi:10.1029/JD094iD06p08599.

Liu, Y., and P. H. Daum, 2004: Parameterization of the autoconversion. Part I: Analytical formulation of the Kessler-type parameterizations. *J. Atmos. Sci.*, **61**, 1539–1548, doi:10.1175/1520-0469(2004)061<1539:POTAPI>2.0.CO;2.

Long, A. B., 1974: Solutions to the droplet collection equation for polynomial kernels. *J. Atmos. Sci.*, **31**, 1040–1052, doi:10.1175/1520-0469(1974)031<1040:STTDCE>2.0.CO;2.

Manton, M. J., and W. R. Cotton, 1977: Formulation of approximate equations for modeling moist deep convection on the mesoscale. Colorado State University Atmospheric Science Paper 266, 62 pp.

Michibata, T., and T. Takemura, 2015: Evaluation of autoconversion schemes in a single model framework with satellite observations. *J. Geophys. Res. Atmos.*, **120**, 9570–9590, doi:10.1002/2015JD023818.

Milbrandt, J. A., and M. K. Yau, 2005: A multimoment bulk microphysics parameterization. Part II: A proposed three-moment closure and scheme description. *J. Atmos. Sci.*, **62**, 3065–3081, doi:10.1175/JAS3535.1.

Morrison, H., J. A. Curry, and V. I. Khvorostyanov, 2005: A new double-moment microphysics parameterization for application in cloud and climate models. Part I: Description. *J. Atmos. Sci.*, **62**, 1665–1677, doi:10.1175/JAS3446.1.

Ogura, Y., and T. Takahashi, 1973: The development of warm rain in a cumulus cloud. *J. Atmos. Sci.*, **30**, 262–277, doi:10.1175/1520-0469(1973)030<0262:TDOWRI>2.0.CO;2.

Onishi, R., K. Matsuda, and K. Takahashi, 2015: Lagrangian tracking simulation of droplet growth in turbulence—Turbulence enhancement of autoconversion rate. *J. Atmos. Sci.*, **72**, 2591–2607, doi:10.1175/JAS-D-14-0292.1.

Pinsky, M., A. Khain, and M. Shapiro, 2001: Collision efficiency of drops in a wide range of Reynolds numbers: Effects of pressure on spectrum evolution. *J. Atmos. Sci.*, **58**, 742–764, doi:10.1175/1520-0469(2001)058<0742:CEODIA>2.0.CO;2.

Pruppacher, H. R., and J. D. Klett, 1997: *Microphysics of Clouds and Precipitation.* Kluwer Academic Publishers, 954 pp.

Seifert, A., and K. D. Beheng, 2001: A double-moment parameterization for simulating autoconversion, accretion and self-collection. *Atmos. Res.*, **59–60**, 265–281, doi:10.1016/S0169-8095(01)00126-0.

——, and ——, 2006: A two-moment cloud microphysics parameterization for mixed-phase clouds. Part 1: Model description. *Meteor. Atmos. Phys.*, **92**, 45–66, doi:10.1007/s00703-005-0112-4.

Shipway, B. J., and A. A. Hill, 2012: Diagnosis of systematic differences between multiple parameterizations of warm rain microphysics using a kinematic framework. *Quart. J. Roy. Meteor. Soc.*, **138**, 2196–2211, doi:10.1002/qj.1913.

Skamarock, W. C., and Coauthors, 2008: A description of the Advanced Research WRF version 3. NCAR Tech. Note TN-475+STR, 113 pp., doi:10.5065/D68S4MVH.

Thompson, G., and T. Eidhammer, 2014: A study of aerosol impacts on clouds and precipitation development in a large winter cyclone. *J. Atmos. Sci.*, **71**, 3636–3658, doi:10.1175/JAS-D-13-0305.1.

——, P. R. Field, R. M. Rasmussen, and W. D. Hall, 2008: Explicit forecasts of winter precipitation using an improved bulk microphysics scheme. Part II: Implementation of a new snow parameterization. *Mon. Wea. Rev.*, **136**, 5095–5115, doi:10.1175/2008MWR2387.1.

Tripoli, G. J., and W. R. Cotton, 1980: A numerical investigation of several factors contributing to the observed variable intensity of deep convection over South Florida. *J. Appl. Meteor.*, **19**, 1037–1063, doi:10.1175/1520-0450(1980)019<1037:ANIOSF>2.0.CO;2.

Wood, R., and P. N. Blossey, 2005: Comments on ''Parameterization of the autoconversion. Part I: Analytical formulation of the Kessler-type parameterizations.'' *J. Atmos. Sci.*, **62**, 3003–3006, doi:10.1175/JAS3524.1.

Zhang, Y., B. Stevens, and M. Ghil, 2005: On the diurnal cycle and susceptibility to aerosol concentration in a stratocumulus-topped mixed layer. *Quart. J. Roy. Meteor. Soc.*, **131**, 1567–1583, doi:10.1256/qj.04.103.